

A Stellar Spectral Flux Library, 1150—25000 Å

A. J. Pickles

Institute for Astronomy, University of Hawaii, Hilo, HI 96720
pickles@ifa.hawaii.edu

ABSTRACT

A stellar spectral flux library of wide spectral coverage, and an example of its application are presented. The new library consists of 131 flux calibrated spectra, encompassing all normal spectral types and luminosity classes at solar abundance, and metal-weak and metal-rich F–K dwarf and G–K giant components. Each library spectrum was formed by combining data from several sources overlapping in wavelength coverage. The SIMBAD database, measured colors and line strengths were used to check that each input component has closely similar stellar type. The library has complete spectral coverage from 1150—10620 Å for all components, and to 25000 Å for about half of them, mainly later types of solar abundance. Missing spectral coverage in the infrared currently consists of a smooth energy distribution formed from standard colors for the relevant types. The library is designed to permit inclusion of additional digital spectra, particularly of non-solar abundance stars in the infrared, as they become available. The library spectra are each given as F_λ vs. λ , from 1150—25000 Å in steps of 5 Å.

A program to combine the library spectra in the ratios appropriate to a selected isochrone is described, and an example spectral component signature of a composite population of solar age and metallicity illustrated. The library spectra and associated tables are available as text files by remote electronic access.

Subject headings: atlases — stars: general — galaxies: stellar content

1. Introduction

There are several published stellar libraries, covering the ultraviolet, optical and infrared spectral ranges. They were obtained with different instrumentation, at different resolutions and spectral sampling and for different purposes, including stellar population synthesis and comparison with theoretical spectral flux calculations. Various groups have successfully used these libraries to suit their programs, either individually or in combinations, as reviewed most recently by Leitherer et al. (1996).

The existing libraries combine considerable utility for specific applications with occasional annoying problems for general use including sometimes: limited coverage of wavelength, spectral type or abundance range, poor or doubtful flux calibration or atmospheric feature removal, and necessity to combine spectra from diverse data sets. The spectral classification of some stars has been refined over the years, leading to slight inconsistencies in libraries which group spectra by stellar type.

Theoretical stellar spectra are often preferred for spectral modeling because of their uniformity and generally more extensive coverage of stellar type, luminosity class, chemical abundance and wavelength range. They may be biased in color and line-strength however: there are many minor contributors to stellar opacity and the emergent spectrum, which usually cannot all be included for the full spectral range because of computational constraints. There are also some systematic effects which are attributable to resolvable differences between theoretical and observed stellar libraries, and to color-temperature (and color-color) calibrations, as reviewed by Charlot, Worthey and Bressan (1996).

For population synthesis in particular, it is sometimes preferable to model the light from a composite stellar population in terms of observable spectra. The utility of observed spectra for this and for checking theoretical flux calibrations depends on extending their coverage of type, luminosity class, abundance and wavelength; all of which can clearly be improved.

The objective here is to provide a flux library of observed spectra representing normal stellar types which is as complete and uniform as presently possible, together with a simple and open mechanism for highlighting deficiencies and extending and improving the database as new observations become available. This was done by selecting what are thought to be the best

observed spectra in each wavelength interval, grouping them by spectral type, luminosity class and abundance (and color and line-strength), resampling them on to the chosen output grid and combining them into final library spectra.

The selected grid of spectral types follows closely the types published by Sviderskiene (1988), which combines extensive spectral energy distribution (SED) data of normal stars on a common system normalized to the energy distribution of Vega (Hayes and Latham 1975). It is extended here to include additional non-solar abundance components where such data exist.

2. Data Sources

The chosen input sources are listed in table 1, which summarizes their spectral type and luminosity class coverage, the number of available spectra and those actually used, their wavelength coverage, resolution and sampling. Based on the available libraries, the output wavelength grid was chosen to be 1150—25000 Å with a sampling interval of 5 Å/pixel and resolution of ~ 500 , which is the highest resolution for which full coverage is available. There are higher resolution source spectra, but not enough to cover the wavelength or abundance range adequately. Higher resolution source spectra were binned and/or filtered to provide a chosen output resolution of about 500 over most of the wavelength range. This resolution is insufficient to adequately measure some fine spectral indices known to discriminate between age and metallicity in composite systems (Rose 1994; Jones and Worthey 1995), but is adequate for resolving many other useful luminosity and metallicity sensitive features (Faber et al. 1985; Pickles and van der Kruit 1990), and the Balmer lines including $H\delta$. Projects requiring higher resolution, particularly around the $\lambda\lambda$ 4000 Å break normally have smaller spectral coverage, and can use higher resolution sources directly.

The spectral combination was done in two stages. Firstly the library was formed from the ultraviolet, optical and near infrared sources in the wavelength range 1150—10620 Å. This library has complete spectral coverage for all components (including metal-weak and metal-rich components) over this wavelength region, and is referred to as UVILIB. Secondly the UVILIB spectra were combined with additional infrared data to a long wavelength limit of 25000 Å, to form what is referred to as the UVKLIB library. Both libraries are referred to collectively as HILIB.

3. Component combination: 1150—10620 Å

All the available digital components were initially assigned to a library component according to their spectral type, luminosity class and chemical abundance. Stellar classifications and component groupings were checked against the SIMBAD database operated at Centre de Données Astronomiques, Strasbourg, France, and from the colors and line strengths measured from the spectra themselves.

For each library component, input spectra were read in and converted if necessary to flux per unit wavelength vs. wavelength. These spectra were binned and filtered if necessary (see table 1) to reduce them to a common resolution of about 500, which is a compromise from among the input data. The input spectra were then normalized to unity at 5556 Å, and inspected for conformity with each other and with an appropriate SED; some spectra were adjusted by division by a smooth curve to remove residual flux calibration errors (see section 3.4). The input spectra were then resampled on to the chosen output grid, combined into final library spectra, and inspected again. Based on this interactive and sometimes iterative analysis, some spectra were adjusted by type slightly (one or two classes) if the measured colors warranted. Additional metal-weak and metal-rich library components were added where sufficient data existed — the GK dwarf and giant branches.

Table 2 lists the final library components by type, together with the number of spectra from each source actually used in the combination. There are potentially nine sources in this wavelength range, although in practice the maximum number of such sources for any library spectrum was 7 (eg. G2 V, see column 2 of table 2). The complete assignment of stars by source, name and type for each library component is summarized in table 3, which is rather extended and available electronically (see section 6).

For the actual combination, multiple spectra from each source were first averaged independently, and their standard deviation calculated. Spectra from each source were then resampled by cubic spline interpolation on to the output wavelength grid 1150—10620 Å, and set zero outside of their valid regions or within atmospheric windows where their definition was poor. The data combination is such that valid (non-zero) contributions from the available (pre-averaged) source components became the output library spectrum in wavelength regions where only one

source exists. Where multiple sources exist, they were averaged and their standard deviation calculated for each wavelength point. Discrepant points were then discarded if necessary and the process repeated. In practice however, discrepant data were avoided by explicitly setting to zero those parts of source spectra which deviated significantly from the appropriate standard spectral energy distribution from Sviderskiene (1988) or Gunn and Stryker (1983), and there were few pixel rejections in the formal combination.

The standard deviation curve associated with each library spectrum is that of the combination of (pre-averaged) sources for wavelengths where multiple sources exist, the standard deviation of the average from one source when there are multiple spectra from only one source, and is zero when only one input spectrum defines the library spectrum. This error curve is tabulated with the library spectra for each wavelength point in the electronic distribution, as are the pre-averaged spectra from each available source (see section 6).

The SM plotting and vector arithmetic package (Lupton and Monger 1997) was used to read, display, filter, spline and combine all data. The SM macros to do this are not included in the electronic distribution, but are available on request from the author if combinations of additional data are desired.

3.1. Sviderskiene

This comprehensive study (Sviderskiene 1988) of the energy distribution of stellar spectra provides the basis of the stellar type component selection presented here. The library consists of 98 spectra covering a wide range of standard spectral types and all luminosity classes at solar abundance, with spectral coverage from 1200—10500 Å in 50 Å steps, and one additional flux point at 12500 Å. The flux library has insufficient resolution (50) for our purposes here, but its scope, consistency and accuracy of energy distribution make it an ideal check on all other input spectra for flux calibration and accuracy. Data from this library was used to provide ultraviolet coverage for some later spectral types lacking IUE data however, as identified in the first digit of column 2 of table 2. The 98 types form the basis for each of the solar abundance components in the HILIB library. This component number has been extended here to 131 by the inclusion of additional metal-weak and metal-rich components where the available data permit; G and K type dwarf and giant spectra.

This library and earlier versions (Straizys and Sviderskiene 1972) are also used to generate and check synthetic photometry of digital spectra of standard stellar types.

3.2. Ultraviolet

The IUE atlas (Heck et al. 1984) of 229 low dispersion spectra from the International Ultraviolet Explorer Satellite provides ultraviolet coverage for earlier spectral types O–F, with some G-type spectra. It covers the wavelength range 1153–3201 Å in 2 Å steps at a resolution of 500. Spectra were combined by type and luminosity into the component types described above, and checked against the reference SED from Sviderskiene (1988). The original spectra were double binned, averaged by type and then gauss filtered slightly to better match the resolution of the adjacent longer wavelength components. The individual RMS errors (averaged over 1150–3200 Å) of the IUE spectral averages by component are generally of the order 1–2%; they are not tabulated here, but are listed in the headers of the appropriate spectral data files contained in the electronic distribution (see section 6).

The earliest (O) type spectra are particularly divergent due to variable amounts of close-in dust absorption. Only spectra which reasonably matched the chosen SED from Sviderskiene (1988) were included. The resultant O5 V, O9 V and O8 III spectra are therefore only broadly representative of the emergent spectra from these classes.

3.3. Optical

The stellar atlas of Gunn and Stryker (1983) contains 175 de-reddened and well calibrated spectra covering all normal spectral types and luminosity classes. The spectral coverage extends from 3160–10620 Å, in steps of 10 Å in the blue and 20 Å in the red. The resolution of 250 is unfortunately lower than desired for full inclusion in this library, but these spectra are used to further check the SED of other components, to bridge the gap 3200–3500 Å where necessary, and sometimes in the red from ~9000–10620 Å. About 20 spectral types were modified (slightly, see table 3) from the original reference to that assigned by SIMBAD. About 5 spectra were not used because of uncertainties in their SED or spectral type. HD11004 is either misclassified or the wrong star was observed.

The line strengths of selected features were mea-

sured for these (and all other input) spectra to group them as metal-weak, solar or metal-rich abundance (see section 3.6 and table 3). A few spectra from this atlas were included in metal-weak and metal-rich components, but most are of solar abundance.

The atlas of Kiehling (1987) contains accurate spectrophotometry of 60 Southern and Equatorial stars of F–M spectral types and all luminosity classes. The wavelength coverage is from 3200–8800 Å in steps of 10 Å, which undersamples the original resolution. All spectra except one are used over their complete wavelength range available, but the atmospheric bands at 6800 and 7500 Å are explicitly set to zero and therefore excluded from the final combination. About 11 spectra were classified as metal-weak or metal-rich in the combination, based on their measured line strengths (see tables 2 and 3).

The library of Jacoby, Hunter and Christian (1984) contains 161 relatively high resolution spectra covering all normal spectral types and luminosity classes. There is some non-solar abundance coverage, with about 22 spectra assigned to metal-weak or metal-rich components. The wavelength coverage is from 3510–7427 Å in steps of 1.4 Å. The data were triple binned and averaged by type. The average spectrum was also slightly gauss filtered prior to combination, so as to match other input sources. The atmospheric bands were explicitly set to zero. About 21 spectral types were changed slightly from the original reference to that assigned by SIMBAD (see table 3).

Each spectrum in the library of Silva and Cornell (1992) is itself a compilation of several observations of stars chosen to be of similar spectral type. It contains 72 standard spectra, covering all spectral types and luminosity classes, and several metal-weak and metal-rich types. The wavelength coverage extends from 3510–8930 Å, but the atmospheric bands at 6800, 7200, 7500 and 8200 Å are explicitly set zero in the original data. Some of the original spectral type and luminosity class assignments conflict with those according to SIMBAD, and these group spectra were not used. About 50 were included where appropriate however, including 14 of non-solar abundance (see tables 2 and 3).

The library of Pickles (1985) is another example where each spectrum is itself a combination of observations of stars of similar types. It contains 48 standard spectra, covering all spectral types and luminosity classes, and several metal-weak and metal-rich types. The wavelength range is from 3600–10000 Å

at 3 Å per step, but is poor in the blue and used here from 3900—10000 Å. The data were double binned prior to combination. Again some types are not used because of apparent mis-typing of some input spectra, or because they fail to adequately match the chosen SED templates. About 34 group spectra were included in the combination, including eight of non-solar abundance (see tables 2 and 3).

Pickles and van der Kruit (1990) presented a stellar flux library formed by combining several of the above sources. This represented an early attempt to build a comprehensive stellar library useful for modeling composite stellar systems, and for generating a spectral representation of isochrone models of single stellar populations. The observations of 15 metal-weak and metal-rich giants in the nuclear bulge of our galaxy are used here to extend the metallicity coverage (and utility) of the present library. The wavelength coverage is from 3800—6800 Å.

3.4. Near infrared

The atlas of Serote Roos, Boisson and Joly (1996) contains high resolution, near infrared flux calibrated spectra of 21 giant and supergiant stars of spectral type G–M, of which about half are super metal rich (SMR). The wavelength coverage is 4800—8920 Å at 0.43 Å/pixel. These data were binned by 10 and slightly gauss filtered to match the output resolution prior to combination. The atlas also contains spectra of 7 dwarf and giant stars of spectral type F–M, observed at lower resolution over the wavelength range 5000—9783 Å at 3.3 Å/pixel. These data were double binned prior to combination.

The atlas of Danks and Dennefeld (1994) provides near infrared coverage of 126 MK standards covering all normal spectral types and luminosity classes, together with a few peculiar stellar spectra. The wavelength coverage is from about 5800—10200 Å at 4 Å/pixel. This library provides good spectral feature definition for many library components not otherwise represented in this wavelength regime, which includes important luminosity and metallicity sensitive features such as the near infrared Na I lines, Ca II triplet, TiO and CN features. The data unfortunately suffer from rather poor flux calibration however. A possible alternate source of digital spectra for normal stellar types in this wavelength regime is the spectrophotometry of 61 O–M stars in the wavelength range 5750—8950 Å (Torres-Dodgen and Weaver 1993). This alternate source has lower spectral resolution, and again

suffers from rather poor flux calibration. The atlas of Danks and Dennefeld (1994) was therefore preferred here because of its greater resolution, wavelength coverage and number of spectra. However each spectrum was divided by a smooth curve prior to combination to force the continuum to match the relevant spectrum from Sviderskiene (1988) or Gunn and Stryker (1983). About 30 spectral types were changed slightly from the original reference to that assigned by SIMBAD, and nine spectra were assigned to non-solar abundance components (see tables 2 and 3).

3.5. Accuracy of the combination

Figure 1 shows an example of the UVILIB spectra, for the G2 dwarf component, and is intended to illustrate the typical ‘best’ and ‘worst’ features of the combination. There are some regions of poor correspondence, eg. that of strong metal and CN absorption blueward of the Ca II K and H lines, and around the Ca II triplet. The first is due to real variation among the input spectra in this narrow region, despite their similarity of type, color and other line strengths: this component therefore represents an ‘average’ of real variation within this wavelength region for this type. The second is possibly due to poor calibration of one input spectrum. Some combinatory improvements could be made by applying more vigorous flux adjustments to more of the input spectra, but the approach adopted is to use most input spectra as published where possible. The generally very high degree of correspondence between the various overlapping components is evident. The RMS errors of the individual averages from each input source are generally better than 2%. The RMS errors of the combination of sources into each library component (which are listed with the library spectra available electronically) are typically 1–2% or better, reflecting the generally high accuracy of the input observations themselves, and the good correspondence achievable between sources, provided that care is taken to combine them accurately by type.

3.6. Line Strengths

Line strengths for all the input and library spectra were measured as Local Equivalent Widths, defined as:

$$LEW = \Delta\lambda (1 - 2 F_{line}/(F_{cb} + F_{cr})) \quad \text{where}$$

F_{line} , F_{cb} and F_{cr} are the average fluxes per unit wavelength within the line region, and pseudo ‘contin-

uum’ regions to the blue and red respectively, and $\Delta\lambda$ is the width of the line region in Å. The bandpasses used and feature strengths measured are listed in tables 4 and 5 (see section 6). Any other desired feature can be readily measured from the digital spectra.

Line strengths of the metallicity sensitive Fe I blends at $\lambda\lambda$ 4385, 5270 and 5330 Å, and of the MgH/Mgb feature at 5180 Å were measured for each input spectrum. The logarithm of the sum of these equivalent widths (in Å) was used to calculate a color-corrected metallicity index [Fe/H] from the calibration described in Pickles and van der Kruit (1990), which follows from that first derived for K giants by Whitford and Rich (1983). This is not intended to be an accurate metallicity calibration for earlier types (or dwarfs). In fact it underestimates metallicity for earlier types, but is satisfactory for measuring relative metallicities at a given temperature and luminosity class, and for sorting the input spectra into three abundance categories: ‘metal-weak’ corresponds to abundance indicator strengths in the range 0.1–0.5 of solar; ‘metal-rich’ corresponds to indicator strengths in the range 2–6 times solar. The estimated metallicities of the three abundance components are listed in table 2 for the dwarf and giant branch components with sufficient source coverage to justify separate abundance classes. The estimated metallicities of other components are also listed, but there are insufficient data to construct components of varied metallicity in other luminosity classes.

Figure 2 shows an example of the metallicity range included among the G–K dwarfs (and giants), where the ‘w’, ‘s’ and ‘r’ G0 V components are shown offset vertically. These three library categories correspond to approximately half-solar, solar and twice solar abundance, although there is some abundance spread included within each component.

4. Component combination: 1150—25000 Å

There are few published digital spectral data between $1.06\mu\text{m}$ and $1.43\mu\text{m}$. Cohen et al. (1995, 1996a and 1996b) have published several absolutely calibrated continuous stellar spectra in the wavelength range $\sim 1\text{--}35\mu\text{m}$, of which about 14 spectra are used here. The resolution is low, but the check on spectral energy distribution invaluable. This absolutely calibrated data was used to bridge the $1.06\text{--}1.43\mu\text{m}$ gap where available. This is presently possible for only 12 components and, as can be seen from the last digit

of the second column of table 2, is actually used for eight components (ie. not used for the M giant components). In these and all other cases a smooth energy distribution was formed over the whole spectral range from ultraviolet to L-band by splining between standard UBVRI-JHKL flux points for each spectral types. One other flux point at $1.04\mu\text{m}$ was included from the pre-formed UVILIB library. The smooth curve generated in this way was displayed and used to check component combination and continuity in the infrared; it agrees gratifyingly well with the absolutely calibrated data when present. The smooth curve was used to bridge the wavelength gap above, to provide normalizing points for the infrared data components, and as the sole infrared component when other data did not exist.

The infrared combination consisted of reading the appropriate UVILIB data, and combining it over the extended wavelength range 1150—25000 Å with available infrared components as listed in the last 4 digits of column 2 of table 2. When these 4 digits are all zero, as happens for about half of them, then the relevant UVKLIB spectrum has no observed infrared extension, and that part of the library spectrum consists solely of the smooth energy distribution matched to standard type colors. The standard color points were formed from the measured UVILIB optical data and from standard infrared color data from Bessell and Brett (1988), Koornneef (1983), Tokunaga (1997), and from Fluks et al. (1994) for the M giants. Table 2 lists the measured synthetic colors for each library spectrum. The standard infrared component color data used to form the smooth energy curve are included as table 6 (see section 6). Most of the metal-weak and metal-rich G–K dwarf and giant components lack infrared data; good abundance resolution is restricted to the UVILIB data. More digital spectra of non-solar abundance stars are needed, particularly at infrared wavelengths.

4.1. Infrared

The atlas of Lancon and Rocca-Volmerange (1992) provides FTS spectra of 84 stars of all spectral types and luminosity classes; the data actually used include the recalibrations from 1996. The wavelength range is large, from $1.43\text{--}2.5\mu\text{m}$ at a resolution of 500. It is the existence of this extensive, well calibrated data set which prompted and enabled this library combination. The data was read as F_ν vs. ν , converted to F_λ vs. λ and normalized at $1.45\mu\text{m}$ to the smooth energy

distribution or data from Cohen et. al. (1995, 1996a, 1996b) where available. Although generally well corrected for atmospheric absorption, some spectra are poorly defined around $1.9\mu\text{m}$ because of strong water absorption during the observation, and were set zero there prior to combination.

The atlas of Dallier, Boisson and Joly (1996) contains medium resolution H-band spectra of 40 stars of all spectral types and luminosity classes, including a few spectra of metal-rich stars. The wavelength range is rather narrow, from $15780\text{--}16420\text{ \AA}$ at either 3 or 6 $\text{\AA}/\text{pixel}$. The spectra were normalized at $1.6\mu\text{m}$ to spectra from Lancon and Rocca-Volmerange (1992), and match this data rather well.

The atlas of Kleinmann and Hall (1986) contains high resolution FTS spectra of 26 stars of spectral type F–M, and all luminosity classes. The wavelength range is from $2.01\text{--}2.41\mu\text{m}$. The data was read as F_ν vs. ν , converted to F_λ vs. λ , quadruple binned and normalized at $2\mu\text{m}$ to data from Lancon and Rocca-Volmerange (1992) or the smooth energy distribution.

Fluks et al. (1994) observed 97 M giant stars in the wavelength range $380\text{--}900\text{ nm}$. The latest types are thermally pulsing, long period variables: by observing them several times each they were able to derive time average spectra. Fluks et al. (1994) also constructed synthetic M giant spectra over the large wavelength interval $99\text{--}12500\text{ nm}$, which are appropriate to a given average effective temperature. Each of the UVKLIB components 95–105 include the appropriate synthetic M0–M10 giant spectra on the MK system from this work. The synthetic spectra match the spectral signatures of the observed spectra from UVILIB very well, but have slightly different optical-infrared colors, with the differences increasing for later types. This may be partly because of detector linearity or dynamic range considerations for these very red stars whose red flux can be hundreds of times larger than their visual flux, or because of differences between average and randomly sampled spectral signatures. The time average spectra are considered superior for population synthesis of composite systems to other observed spectra, which sample these late-type, variable stars at random phases. The UVKLIB data therefore include a combination of the observed UVILIB spectra and synthetic spectra in the wavelength range $1150\text{--}10500\text{ \AA}$, and synthetic spectra alone to longer wavelengths. These are the only components whose spectra differ in this wavelength range between UVILIB and UVKLIB.

Figure 3 shows an example of the UVKLIB spectral combination for the K5 giant component, which illustrates the good match between the various infrared components, including the smooth fit between flux points, which represent mean fluxes within the relevant filter pass bands.

Figure 4 shows five example giant spectra from the UVKLIB library, illustrating the detail and wavelength coverage achieved, the spectral bridging between $1.05\text{--}1.43\mu\text{m}$, and the additional coverage provided for the M giants by the spectra from Fluks et al. (1994).

5. Digital Filter Photometry

Magnitude measurements were made from the flux-calibrated digital spectra by convolving them with appropriate filter transmission profiles. In this case, the library spectra are arbitrarily normalized to unity around 5556 \AA , so the magnitude measurements are relative. If T_a and $ZERO_a$ are the transmission profile and magnitude zero point for filter ‘a’, then:

$$MAG_a = -2.5 \text{Log}_{10} \langle F_\nu \rangle - ZERO_a \quad \text{where}$$

$$\langle F_\nu \rangle = \Sigma (T_a F_\nu \Delta\nu) / \Sigma (T_a \Delta\nu) \quad \text{and}$$

$$\langle F_\lambda \rangle = \Sigma (T_a F_\lambda \Delta\lambda) / \Sigma (T_a \Delta\lambda).$$

$$\text{Since } F_\nu d\nu = F_\lambda d\lambda \quad \text{and} \quad d\nu = c d\lambda/\lambda^2,$$

$$\langle F_\nu \rangle = \Sigma (T_a F_\lambda \Delta\lambda) / \Sigma (T_a c \Delta\lambda/\lambda^2)$$

where the last summation formula over wavelength steps is the way $\langle F_\nu \rangle$ and hence filter magnitudes are calculated here, and

$$\langle \lambda_a \rangle = \Sigma (F_\lambda T_a \lambda \Delta\lambda) / \Sigma (F_\lambda T_a \Delta\lambda)$$

is the effective wavelength of filter ‘a’. Color measurements were made by differencing these filter magnitudes, and the synthetic colors then compared to observed or standard colors for each stellar type.

5.1. Filter Transmission Profiles and Zero Points

Filter profiles for Johnson system colors UBV are taken from Buser (1978) for the U3 filter, and from Azusienis and Straizys (1969) for filters B3 and V. The same V filter profile is also used for Kron-Cousins system colors, and the R_c and I_c filter profiles are taken from Bessell (1979). The magnitude zero points for these filters were calculated by digitally photometering the standard spectra from Sviderskiene (1988)

and minimizing the deviations of the measured colors from standard spectral type UVB colors listed in Buser (1978) and BVRI colors listed in Cousins (1981).

Transmission profiles for filters JHKLL' and M are from Bessell and Brett (1988). Zero points for these colors were derived simply by requiring the measured infrared colors of the A0 V library spectrum to be zero, and are very close to those published in Bessell and Brett (1988).

The optical filter transmission profiles are tabulated in table 7, and those for the infrared filters in table 8 (see section 6). Filter zero points used here are: U3 (0.697); B3 (-0.109); V (0.0); R_c (0.159) I_c (0.388); J (0.884); H (1.365); K (1.868); L (2.744); L' (2.941); M (3.389).

5.2. Library coverage in the HR diagram

The synthetic colors measured from the library spectra are listed in columns 5–11 of table 2, Component temperatures listed in column 4 were assigned by reference to these colors (V-I_c and especially V-K) and Bessell (1979), Tokunaga (1997), and to Fluks et al. (1994) for the M giant stars. The resulting V-K vs. Log T_e calibration, shows strong separation between dwarf and giant branches for M types, with M giants becoming increasingly redder with later type than dwarfs of similar effective temperature. This is noticeably different from the color-temperature relation used for late giants by Bertelli et al. (1994) for example. Their giant branch calibration bisects the dwarf and giant relationships here, and is in fact closer to the dwarf relation for their latest type M giants. The effect of this difference on predicted colors of composite systems is followed in section 7.

Component bolometric corrections listed in column 14 are also assigned by reference to Bessell and Wood (1984) for most types with $V - I_c > 0$, to Lang (1992) for earlier types, and to Fluks et al. (1994) and Fluks et al. (1997), which includes absolute calibrations derived from HIPPARCOS data, for the M giant components. The temperature assignments determine the placement of components in the temperature-luminosity plane when constructing spectra appropriate to a given stellar population (see section 7). Similarly the bolometric corrections determine the light fractions assigned to each library component in this procedure. The bolometric magnitudes listed in column 13 are of lesser importance

here, since they are adjusted to match the selected isochrone values, and are assigned here to match the solar-age, solar abundance isochrone from Bertelli et al. (1994).

Figure 5 shows the library points overplotted as bolometric magnitude vs. Log T_e on a sample solar-abundance, 5 Gyr isochrone from Bertelli et al. (1994). This figure shows the good coverage of most evolutionary stages within this plane provided by the spectral library. The library does not contain spectra to match the latest white dwarf stages of evolution, but these are minority components within this wavelength range, and can be well represented by black body spectra.

Figure 6 illustrates the metallicity coverage available for the main sequence turnoff, subgiant and early giant branch regions. Solar age isochrones of approximately half-solar, solar and twice solar abundance from Bertelli et al. (1994) are plotted as absolute magnitude vs. V-I_c color. The available library points of different metallicities are overlaid to illustrate the range (and the limits) of metallicity coverage afforded by the library spectra.

6. Electronic Distribution

The electronic distribution of this data includes additional tables detailing: the source spectra and classifications for each library component (table 3), the bandpasses used for measuring line equivalent widths (table 4) and the measured equivalent widths (table 5), the standard component infrared color data used to form the smooth infrared energy distributions (table 6) and the filter transmission curves used for the digital photometry (tables 7 and 8).

The UVILIB spectral library consists of 131 text files arranged in 5–10 columns, depending on the number of input components. Each file lists wavelength from 1150–10620 Å at 5 Å/pixel steps in the first column, the corresponding F_λ in column 2, the standard deviation of the optical combination in column 3, and the source contributions in subsequent columns, identified by the same lettering as used in table 2. The normalized source contributions are averages where multiple components from a source exist. The first of three header lines summarizes RMS errors of these individual averages. The standard deviation column is generally zero in wavelength regions where only one source is present, but is sometimes replaced by the standard deviation of the average forming that

single component.

The UVKLIB spectral library also consists of 131 text files arranged in 5–8 columns. Each file lists wavelength from 1150–25000 Å, at 5 Å/pixel steps in the first column, the corresponding F_λ in column 2, the standard deviation of the combination in column 3, the spectrum from UVLIB (above) in column 4, and the infrared source spectra in subsequent columns.

7. MASPS: Make A Stellar Population Spectrum

The new library was constructed to enable detailed spectral modeling from the ultraviolet to the infrared of the emergent flux from a composite stellar system. A brief description of this application and an example are illustrated here.

An interactive C program has been written to read a selected isochrone from the extensive compilation of Bertelli et al. (1994), co-add library spectra in the ratios appropriate to the selected isochrone and a chosen mass function, and hence derive a realistic spectral representation of the emergent spectrum from a coeval stellar population of given age, metallicity and initial mass function. The steps involved are:

- (1) Select and read the Evolutionary points (EPs) of the chosen Isochrone (Age, Metallicity). Each EP represents the point reached in the temperature-luminosity plane of a star of given initial mass. The isochrone tabulation lists for each EP: Age, initial mass, temperature, bolometric and visual magnitudes, U-B, B-V, V- R_c , V- I_c , V-J, V-H and V-K colors. There are typically about 160 EPs in an isochrone tabulation from Bertelli et al. (1994).

- (2) Extrapolate the EPs to lower masses. Typically the isochrone tabulation extends to a lower mass of about $0.6 M_\odot$; this needs to be extended to a chosen lower mass cut-off (typically $0.15 M_\odot$) to properly account for lower main sequence starlight. The extrapolation is linear in $\text{Log } T_e$. The latest type dwarf spectrum contained in the library is M6 V, which corresponds to stars more massive than this limit. Although the lowest mass stars contribute significantly to the mass of the composite system, they contribute very little to the emergent flux at any wavelength. Additional spectra of later type dwarfs would enhance the library's completeness, but in fact would have negligible impact on the emergent flux.

- (3) Choose a mass function. This could be a power-

law function where a slope of $s=2.35$ would represent a Salpeter (1955) initial mass function: this produces dwarf mass contributions (and hence M/L ratio) which increase rapidly with decreasing low-mass cutoff, although the resultant spectrum and colors are relatively insensitive to this limit within reasonable bounds. Alternatively, and as shown here, a Miller and Scalo (1979) mass function can be used: this is much less sensitive to an arbitrary low-mass cutoff and gives lower M/L ratios, but in fact produces very similar spectra. The chosen initial mass function determines the number of stars at each EP, and enables calculations of the total population colors from the color transformations used by Bertelli et al. (1994).

- (4) Select the UVKLIB spectra which most closely emulate the isochrone EPs in temperature, gravity and abundance. In practice this means choosing dwarf and giant spectra of a given metallicity: metal-weak, metal rich or solar abundance; restricting the dwarf components to those appropriate to the extent of the chosen isochrone main sequence; choosing the appropriate subgiant components and matching giant components to the first, second and possibly third isochrone giant branch evolutionary tracks. Some important phases (eg. at the beginning and end of evolutionary changes) are best represented by fractional UVKLIB spectra, which are interpolated in $\text{Log } T_e$ from the adjacent spectra. There are typically about 60 spectral components selected this way. Some post asymptotic giant branch components can be represented by appropriate library components, but most (eg. White Dwarfs) require computation of black-body spectra appropriate to the EP temperature.

- (5) Match the chosen spectra to (groups of) the EPs. In practice this means varying the bolometric magnitudes of the chosen spectra while maintaining their temperatures so that they slide vertically in the temperature-luminosity plane. The temperature and bolometric corrections assigned to each library spectrum are functions of their color, metallicity and luminosity class, and should remain constant as age varies. The bolometric magnitudes assigned in table 2 are indicative values for approximately solar age and metallicity, but are varied arbitrarily here to match different isochrones.

- (6) Interpolate the stellar numbers from the EPs to the library components, again using the chosen mass function to determine initial mass intervals between the library components. The Visual light from each component can then be calculated from the bolomet-

ric magnitude appropriate to the isochrone, the assigned bolometric correction, and the relative number of stars.

(7) Combine the library spectra in the ratios determined above to produce a spectrum appropriate to the chosen isochrone and mass function. The colors of the composite spectrum now depend on the library spectra colors and their effective temperature and bolometric correction assignments. These composite spectrum colors can be measured and compared with those predicted in step 3 above from the isochrone EPs and color transformation of Bertelli et al. (1994).

In principle, the transformation from the theoretical plane (luminosity and effective temperature) to the observed plane (magnitude and color), and the corresponding reverse transformation, should be symmetric. As described in section 5.2 however, these calibrations are different and need to be resolved to remove an important source of uncertainty in the modeling of composite system colors. The optical-infrared colors of the composite library spectrum derived here are redder than those predicted by Bertelli et al. (1994) because of this difference in color-temperature calibration. Work in progress should help to resolve this difference (eg. Fluks et al. 1997).

Figure 7 shows the solar-age, solar abundance isochrone with the library component flux points overplotted at their fixed temperatures and adjusted bolometric magnitudes, and sized according to (a) the V-light fractions and (b) the K-light fractions emitted by each component. This diagram illustrates schematically the relative contributions of different stellar components, and can be displayed for any wavelength.

Figure 8 shows the composite spectrum obtained by co-adding the library components in the ratios determined by this procedure. The lower traces show how the partial contributions of significant evolutionary phases vary in importance with wavelength, and the upper trace shows the emergent spectrum appropriate to the (assumed single-burst) stellar population. This diagram illustrates the coverage and detail of the spectral representation which can be obtained with the new library.

8. Summary

Available published spectra have been combined to provide a new library of digital stellar spectra which combines reasonable resolution with wide wavelength

coverage in the range 1150—25000 Å. The library covers all normal spectral types and luminosity classes, and provides some abundance resolution among G–K dwarfs and giants, and is amenable to future extension. More spectra are desirable, particularly of non-solar abundance stars in the infrared. The spectra and associated tabular data are available by remote electronic access.

The library has been constructed to enable synthesis and modeling of the integrated light from composite populations. The library spectra can be combined in proportions determined by the kind of detailed isochrone tabulations of stellar systems now available (eg. Bertelli et al. 1994) to produce a spectral (color and line strength) representation of any composite stellar system. There are differences, which should soon be resolved, in the color-temperature relations, with the library M giant spectra being redder in V–K for a given effective temperature than tabulated in Bertelli et al. (1994).

Composite spectra of similar detail to the example shown can be constructed for any age and some abundances. Such spectra can be used to measure the detailed variation of spectral signature, color and line strength with metallicity and age of star formation, and to synthesize observed spectra and associated photometry of galaxies. The detailed variation of spectral signature as a function of age and metallicity will be the subject of another paper.

We are grateful to the observers and authors of the data which are combined here, to the staff of the Astronomical Data Center (Goddard Space Flight Center) and to the staff of SIMBAD and the Centre de Données Astronomiques de Strasbourg for enabling access to it and the on-line databases used here.

TABLE 1
STELLAR LIBRARY INPUT SOURCE SUMMARY

	Spectral Types	Luminosity Classes	$N_{avail}/$ N_{used}	$\lambda\lambda$ Range Å	R	Å/ Pixel	\times Bin ^a	Usage	ref
SVID ^b	O–M	I–V	98/98	1200 — 10500	50	50	-	SED, uv for late types	1
IUE	O–G	I–V	229/173	1153 — 3201	500	2	2	uv for early types	2
GS	O–M	I–V	175/170	3160 — 10620	250	10/20	-	3200—3500 Å, 9000—10620 Å	3
KIEHL	F–M	I–V	60/59	3200 — 8800	500	10	-	where available	4
JHC	O–M	I–V	161/157	3510 — 7427	1200	1.4	3	where available	5
SC	O–M	I–V	72/52	3510 — 8930	500	5	-	some doubtful types excluded	6
PIC	O–M	I–V	48/34	3600 — 10000	500	3	2	3900 — 10000 Å	7
N6522	K	III	16/15	3800 — 6800	400	6	-	where available	8
SRBJ	GKM	I/III	21/19	4800 — 8920	6000	0.43	10	where available	9
SRBJ	GKM	I/III	7/7	5000 — 9783	1000	3.3	2	where available	9
DD	O–M	I–V	130/121	5804 — 10200	800	4	-	contin. fitted to SVID or GS	10
LRV	O–M	I–V	84/83	14300 — 25000	500	~7	-	where available	11
DBJ	O–M	I,III,V	40/36	15700 — 165000	2000	3/6	2/1	where available	12
KH	F–M	I–V	26/24	20100 — 24100	3000	~2	4	contin. fitted to LRV or COHEN	13
COHEN	AGKM	III,V	14/8	10000 — 350000	100	100	-	where available	14
FLUKS	M	III	11/11	995 — 125000	5000	1	8	Synthetic MIII spectra	15

^aBinning of data prior to combination; the IUE, JHC and higher resolution SRBJ data were also slightly gauss filtered to match other data sets and conform to the chosen output resolution.

^bSVID spectra were used to define the Spectral Energy Distribution (SED) for most types and to check other input spectra flux calibrations. They were included in the final combination when no other spectra were available; the uv of some late types, and a few other gaps.

References.— (1) Sviderskiene (1988); (2) Heck et al. (1984); (3) Gunn and Stryker (1983) (4) Kiehling (1987); (5) Jacoby, Hunter and Christian (1984); (6) Silva and Cornell (1992); (7) Pickles (1985); (8) Pickles and van der Kruit (1990); (9) Serote Roos, Boisson and Joly (1996); (10) Danks and Dennefeld (1994); (11) Lancon and Rocca-Volmerange (1992); (12) Dallier, Boisson and Joly (1996); (13) Kleinmann and Hall (1986); (14) Cohen et al. (1995, 1996a, 1996b); (15) Fluks et al. (1994)

TABLE 2
 STELLAR LIBRARY COMPONENTS, PHYSICAL DATA, SYNTHETIC PHOTOMETRY

N	Components ^a			Type ^c	Log T _e	U ₃ -V	B ₃ -V	V-R _c	V-I _c	V-J	V-H	V-K	[Fe/H] ^d	M _{bol}	BC _V ^e
	b _{sigk}	jspnrd	ldkc												
1	1710	310002	3000	O5 V	4.600	-1.48	-0.38	-0.17	-0.36	-0.74	-0.99	-1.10	0	-8.9	-3.7
2	1310	600001	2100	O9 V	4.550	-1.39	-0.33	-0.19	-0.35	-0.72	-0.90	-0.99	0	-7.8	-3.3
3	1210	210001	1100	B0 V	4.450	-1.33	-0.34	-0.16	-0.31	-0.70	-0.83	-0.86	0	-5.9	-2.4
4	1710	101003	0000	B1 V	4.350	-1.14	-0.24	-0.12	-0.24	-0.63	-0.73	-0.78	0	-4.7	-2.0
5	1720	400011	1200	B3 V	4.280	-0.86	-0.20	-0.10	-0.15	-0.48	-0.73	-0.80	0	-3.5	-1.5
6	2720	200011	0000	B57 V	4.150	-0.55	-0.14	-0.07	-0.08	-0.32	-0.37	-0.40	0	-2.7	-1.0
7	1610	000001	0000	B8 V	4.070	-0.34	-0.11	-0.03	-0.06	-0.23	-0.26	-0.28	0	-2.1	-0.6
8	1310	001001	0000	B9 V	4.030	-0.20	-0.04	-0.02	-0.04	-0.14	-0.15	-0.16	0	-1.0	-0.34
9	1420	211001	1002	A0 V	3.980	0.04	0.02	-0.01	0.01	0.00	0.00	-0.01	0	0.3	-0.18
10	1210	300002	1000	A2 V	3.950	0.10	0.03	0.01	0.05	-0.02	-0.15	-0.14	0	1.1	-0.08
11	1520	110000	1000	A3 V	3.944	0.15	0.09	0.04	0.10	0.04	-0.13	-0.13	0	1.3	-0.03
12	1430	101001	0000	A5 V	3.929	0.24	0.15	0.05	0.16	0.29	0.35	0.36	0	1.7	0.01
13	1260	210002	0000	A7 V	3.906	0.30	0.20	0.11	0.24	0.37	0.46	0.47	0	2.1	0.01
14	1431	300010	0000	F0 V	3.858	0.35	0.30	0.18	0.38	0.53	0.66	0.68	0	3.0	0.02
15	1210	101002	2000	F2 V	3.831	0.39	0.40	0.21	0.46	0.61	0.62	0.65	0	3.3	0.03
16	1120	311000	2000	F5 V	3.815	0.42	0.46	0.24	0.50	0.83	1.03	1.06	0.0	3.5	0.00
17	1110	210000	0000	wF5 V	3.820	0.35	0.44	0.25	0.51	0.78	1.01	1.04	-0.3	3.8	-0.02
18	1122	210003	2010	F6 V	3.798	0.48	0.47	0.27	0.56	0.90	1.11	1.13	0.0	3.8	-0.03
19	1110	110000	0000	rF6 V	3.786	0.56	0.51	0.30	0.60	0.95	1.21	1.24	0.3	3.3	-0.04
20	1120	410000	3100	F8 V	3.781	0.60	0.54	0.30	0.62	1.01	1.22	1.25	0.0	4.0	-0.04
21	1120	211000	0000	wF8 V	3.788	0.53	0.52	0.29	0.59	0.96	1.26	1.29	-0.6	4.3	-0.05
22	1111	200000	0000	rF8 V	3.761	0.68	0.57	0.33	0.68	1.05	1.36	1.39	0.2	3.7	-0.06
23	1120	101001	2100	G0 V	3.764	0.69	0.57	0.32	0.67	1.02	1.28	1.30	0.0	4.2	-0.04
24	1120	110000	0000	wG0 V	3.767	0.65	0.55	0.32	0.66	0.97	1.31	1.35	-0.8	4.7	-0.05
25	1110	210000	0000	rG0 V	3.751	0.77	0.59	0.35	0.72	1.08	1.40	1.44	0.4	3.8	-0.08
26	1112	210011	2021	G2 V	3.751	0.81	0.63	0.35	0.72	1.21	1.54	1.56	-0.2	4.6	-0.10
27	1110	101001	2000	G5 V	3.747	0.95	0.69	0.36	0.74	1.19	1.45	1.51	0.0	4.7	-0.08
28	1112	120000	0000	wG5 V	3.760	0.77	0.65	0.35	0.69	1.15	1.47	1.54	-0.4	5.0	-0.07
29	1111	110000	0000	rG5 V	3.748	1.00	0.70	0.38	0.73	1.22	1.58	1.63	0.1	3.9	-0.10
30	3021	220000	2100	G8 V	3.727	1.13	0.75	0.41	0.81	1.34	1.69	1.76	0.4	5.1	-0.14
31	3020	001001	0100	K0 V	3.715	1.20	0.77	0.45	0.87	1.38	1.83	1.90	0.1	5.4	-0.18
32	3011	010020	2210	rK0 V	3.719	1.40	0.83	0.46	0.85	1.50	1.96	2.02	0.5	4.7	-0.20
33	1120	001001	0200	K2 V	3.689	1.58	0.92	0.52	0.97	1.65	2.14	2.23	0	5.9	-0.29
34	3010	010010	1100	K3 V	3.653	1.73	0.93	0.60	1.11	1.81	2.37	2.40	0	6.4	-0.40
35	3021	101000	0000	K4 V	3.638	1.95	1.09	0.66	1.23	1.97	2.54	2.64	0	6.7	-0.51
36	3010	000000	0000	K5 V	3.622	2.34	1.21	0.75	1.36	2.17	2.77	2.87	0	7.0	-0.64
37	3040	200000	2100	K7 V	3.602	2.46	1.37	0.83	1.58	2.40	2.97	3.09	0	7.4	-0.81
38	3010	000001	0000	M0 V	3.580	2.51	1.32	0.86	1.71	2.86	3.51	3.68	0	7.5	-1.12
39	4000	001011	0000	M1 V	3.566	2.58	1.38	0.88	1.87	2.97	3.62	3.90	0	7.8	-1.25
40	3020	010001	1010	M2 V	3.550	2.50	1.44	0.96	2.02	3.29	3.96	4.14	0	8.1	-1.48
41	3000	001001	0200	M2.5 V	3.537	2.67	1.50	1.02	2.25	3.56	4.20	4.41	0	8.4	-1.71
42	3010	210000	0000	M3 V	3.519	2.57	1.52	1.07	2.44	3.82	4.45	4.67	0	8.7	-1.93
43	3010	001000	0000	M4 V	3.493	3.01	1.59	1.22	2.78	4.42	5.04	5.31	0	9.1	-2.44
44	3010	001000	1010	M5 V	3.470	3.02	1.66	1.37	3.14	5.25	6.10	6.39	0	9.5	-3.22
45	3010	000000	0000	M6 V	3.431	3.05	1.82	1.65	3.69	6.36	7.03	7.41	0	10.0	-4.2
46	0220	000011	0100	B2 IV	4.300	-1.15	-0.30	-0.13	-0.24	-0.62	-0.72	-0.74	0	-4.6	-1.9
47	0420	000000	0000	B6 IV	4.100	-0.42	-0.11	-0.04	-0.09	-0.32	-0.42	-0.45	0	-2.4	-0.8
48	0430	000001	0000	A0 IV	3.988	-0.01	-0.05	-0.01	-0.00	-0.02	-0.02	-0.03	0	-0.1	-0.2
49	0220	010000	0000	A47 IV	3.900	0.17	0.08	0.04	0.09	0.28	0.39	0.38	0	1.1	-0.00
50	1330	210002	0000	F02 IV	3.847	0.36	0.34	0.20	0.41	0.59	0.70	0.74	0	2.0	0.03
51	1121	000002	1000	F5 IV	3.817	0.42	0.40	0.24	0.50	0.80	0.97	0.98	0	2.3	-0.01
52	3002	010002	1010	F8 IV	3.789	0.66	0.55	0.29	0.59	1.03	1.28	1.29	0	2.7	-0.03
53	3010	110010	0000	G0 IV	3.773	0.79	0.59	0.32	0.64	1.01	1.40	1.39	0	3.2	-0.04
54	3050	110001	0100	G2 IV	3.755	0.97	0.68	0.34	0.70	1.11	1.40	1.50	-0.1	3.1	-0.05
55	3021	111010	0000	G5 IV	3.748	1.13	0.75	0.39	0.77	1.21	1.51	1.60	0.1	3.1	-0.08
56	3030	001001	1000	G8 IV	3.725	1.37	0.82	0.45	0.86	1.40	1.74	1.80	-0.4	3.1	-0.15
57	3030	000001	0000	K0 IV	3.700	1.65	0.95	0.51	0.96	1.42	1.91	1.99	0.0	2.9	-0.21
58	3020	000000	0000	K1 IV	3.680	1.71	1.07	0.56	1.04	1.53	2.01	2.10	-0.3	2.8	-0.27
59	3040	000000	0000	K3 IV	3.660	2.34	1.18	0.62	1.17	1.83	2.32	2.41	0.0	2.6	-0.39
60	1200	510001	0000	O8 III	4.500	-1.40	-0.34	-0.16	-0.35	-0.82	-0.83	-0.95	0	-8.7	-3.1
61	1620	200003	0200	B12 III	4.300	-1.18	-0.26	-0.14	-0.24	-0.53	-0.62	-0.72	0	-5.9	-1.8
62	1310	200001	0000	B3 III	4.230	-0.85	-0.19	-0.12	-0.16	-0.52	-0.52	-0.54	0	-4.6	-1.4
63	1410	300003	0000	B5 III	4.170	-0.63	-0.15	-0.08	-0.10	-0.32	-0.42	-0.44	0	-3.5	-1.01
64	1410	300004	0000	B9 III	4.045	-0.17	-0.08	-0.03	-0.06	-0.12	-0.22	-0.23	0	-1.3	-0.39
65	1110	100001	0000	A0 III	3.981	0.04	0.04	0.00	0.01	-0.02	-0.02	-0.04	0	-0.4	-0.29

TABLE 2—*Continued*

N	Components ^a			Type ^c	Log T _e	U ₃ -V	B ₃ -V	V-R _c	V-I _c	V-J	V-H	V-K	[Fe/H] ^d	M _{bol}	BC _V ^e
	b _{sigk}	jspnrd	ldkc												
66	1100	200001	1000	A3 III	3.953	0.24	0.13	0.05	0.08	0.08	-0.05	-0.08	0	0.3	0.08
67	1110	100000	0000	A5 III	3.927	0.28	0.18	0.07	0.16	0.29	0.39	0.38	0	0.5	0.04
68	1300	110002	2000	A7 III	3.906	0.35	0.21	0.12	0.24	0.40	0.28	0.38	0	1.0	0.05
69	1211	101002	0000	F0 III	3.880	0.39	0.27	0.14	0.32	0.49	0.69	0.68	0	1.1	0.05
70	3000	100001	0000	F2 III	3.835	0.45	0.42	0.23	0.45	0.69	0.80	0.79	0	1.6	0.03
71	1101	411002	0000	F5 III	3.815	0.49	0.43	0.25	0.51	0.80	1.09	1.08	0	1.6	-0.02
72	3001	210000	1120	G0 III	3.749	0.94	0.66	0.37	0.73	1.31	1.74	1.76	-0.22	2.0	-0.13
73	3002	101011	3110	G5 III	3.713	1.45	0.89	0.45	0.87	1.54	2.01	2.05	-0.12	3.2	-0.21
74	3020	210001	0000	wG5 III	3.715	1.19	0.81	0.45	0.86	1.47	1.91	2.00	-0.26	2.8	-0.20
75	3002	200111	0000	rG5 III	3.709	1.43	0.87	0.47	0.89	1.62	2.11	2.21	0.23	3.4	-0.25
76	3010	310012	1110	G8 III	3.700	1.63	0.95	0.48	0.93	1.59	2.07	2.12	0.06	3.1	-0.24
77	3010	001111	0000	wG8 III	3.701	1.51	0.87	0.47	0.92	1.52	2.01	2.10	-0.38	2.7	-0.23
78	3020	001001	2121	K0 III	3.686	1.80	0.96	0.50	0.98	1.69	2.19	2.25	-0.08	3.1	-0.29
79	3020	000301	0000	wK0 III	3.697	1.53	0.95	0.48	0.94	1.62	2.11	2.20	-0.33	2.5	-0.26
80	3020	100001	0000	rK0 III	3.683	1.90	1.00	0.52	0.99	1.77	2.31	2.40	0.18	3.3	-0.33
81	3030	000001	2000	K1 III	3.668	1.99	1.04	0.54	1.04	1.82	2.33	2.41	0.09	1.8	-0.36
82	3030	001001	0000	wK1 III	3.683	1.84	1.02	0.52	0.99	1.77	2.32	2.41	-0.10	1.2	-0.33
83	3011	001210	0000	rK1 III	3.662	2.25	1.10	0.56	1.07	1.93	2.51	2.61	0.27	3.2	-0.43
84	3020	010001	2012	K2 III	3.649	2.14	1.11	0.59	1.13	1.97	2.62	2.67	0.05	0.9	-0.47
85	3020	000101	0000	wK2 III	3.666	2.06	1.04	0.54	1.05	1.92	2.51	2.60	-0.38	0.7	-0.42
86	3001	320011	0000	rK2 III	3.648	2.38	1.19	0.60	1.14	2.08	2.72	2.81	0.24	2.5	-0.52
87	3010	001001	1211	K3 III	3.640	2.44	1.21	0.62	1.17	2.22	2.95	3.11	-0.02	0.5	-0.63
88	3020	001100	0000	wK3 III	3.645	2.17	1.14	0.60	1.16	2.12	2.81	2.90	-0.36	-0.2	-0.57
89	3031	100320	0000	rK3 III	3.641	2.72	1.31	0.64	1.20	2.28	2.97	3.12	0.27	1.6	-0.65
90	3020	101000	1100	K4 III	3.626	2.98	1.43	0.71	1.34	2.42	3.21	3.38	0.09	-0.5	-0.79
91	3030	001000	0000	wK4 III	3.628	2.75	1.34	0.70	1.32	2.33	3.02	3.22	-0.33	-1.0	-0.73
92	3011	111200	0000	rK4 III	3.626	2.80	1.41	0.71	1.34	2.49	3.22	3.42	0.15	0.6	-0.83
93	3030	001002	3311	K5 III	3.603	3.07	1.42	0.78	1.54	2.67	3.40	3.57	-0.09	-1.3	-0.98
94	3020	011111	0000	rK5 III	3.601	3.24	1.50	0.81	1.57	2.75	3.53	3.72	0.08	-0.3	-1.05
95	1031	100000	0010	M0 III ^f	3.582	3.02	1.43	0.80	1.65	2.81	3.68	3.81	0	-1.9	-1.24
96	1001	011010	0110	M1 III ^f	3.577	3.01	1.44	0.83	1.76	2.97	3.87	3.99	0	-2.1	-1.38
97	1010	000001	1010	M2 III ^f	3.569	3.05	1.45	0.87	1.86	3.13	4.05	4.23	0	-2.3	-1.53
98	1032	110001	4100	M3 III ^f	3.560	2.95	1.43	0.91	2.08	3.44	4.36	4.54	0	-2.5	-1.81
99	1032	110010	2000	M4 III ^f	3.551	2.80	1.40	0.99	2.39	3.95	4.88	5.07	0	-2.8	-2.26
100	1031	210002	3010	M5 III ^f	3.534	2.39	1.29	1.11	2.77	4.66	5.62	5.84	0	-3.0	-2.92
101	1021	111001	0000	M6 III ^f	3.512	2.09	1.23	1.33	3.22	5.55	6.58	6.79	0	-3.5	-3.78
102	1030	000001	1020	M7 III ^f	3.495	1.43	1.09	1.65	3.81	6.76	7.82	8.05	0	-3.8	-4.95
103	1020	000001	2000	M8 III ^f	3.461	1.05	1.16	1.85	4.11	8.04	9.08	9.36	0	-4.2	-6.15
104	0000	000000	0000	M9 III ^f	3.426	0.96	1.17	1.68	3.86	8.04	8.97	9.33	0	-4.6	-6.09
105	0000	000000	0000	M10 III ^f	3.398	0.73	1.03	1.67	3.98	8.33	9.11	9.58	0	-5.0	-6.35
106	1300	100001	0000	B2 II	4.204	-1.06	-0.17	-0.12	-0.22	-0.39	-0.42	-0.43	0	-6.0	-1.2
107	1100	000001	0000	B5 II	4.100	-0.75	-0.12	-0.06	-0.15	-0.16	-0.15	-0.15	0	-5.0	-0.9
108	3001	100001	0000	F0 II	3.900	0.34	0.15	0.09	0.20	0.44	0.59	0.62	0	-2.5	0.09
109	3002	100002	0000	F2 II	3.865	0.54	0.34	0.18	0.36	0.52	0.69	0.73	0	-2.4	0.09
110	3003	200002	0000	G5 II	3.720	1.44	0.90	0.44	0.84	1.31	1.71	1.80	-0.0	-2.6	-0.12
111	4001	000011	0001	K01 II	3.700	2.51	1.27	0.59	1.09	1.72	2.10	2.21	-0.2	-2.8	-0.31
112	3002	000002	0001	K34 II	3.629	3.11	1.42	0.70	1.32	2.37	3.05	3.16	0.1	-3.1	-0.73
113	3002	000000	1000	M3 II	3.533	3.45	1.65	1.04	2.29	3.78	4.70	5.00	0	-4.1	-1.96
114	1510	200001	0000	B0 I	4.415	-1.22	-0.22	-0.13	-0.22	-0.57	-0.61	-0.71	0	-8.9	-1.8
115	1300	510000	1100	B1 I	4.316	-1.11	-0.17	-0.08	-0.16	-0.47	-0.59	-0.67	0	-8.3	-1.6
116	1100	210002	0000	B3 I	4.193	-0.90	-0.15	-0.05	-0.13	-0.30	-0.33	-0.30	0	-7.6	-1.18
117	1210	200002	0000	B5 I	4.127	-0.77	-0.06	-0.03	-0.01	-0.16	-0.15	-0.16	0	-7.2	-0.88
118	1410	100001	1000	B8 I	4.049	-0.58	-0.01	-0.03	0.03	-0.04	-0.09	-0.04	0	-6.9	-0.26
119	1100	300001	0000	A0 I	3.988	-0.24	0.00	0.02	0.07	0.10	0.19	0.16	0	-6.7	-0.18
120	1400	100001	0000	A2 I	3.958	-0.13	0.10	0.06	0.12	0.20	0.32	0.30	0	-6.7	-0.04
121	1402	400003	1000	F0 I	3.886	0.43	0.20	0.12	0.31	0.44	0.56	0.58	0	-6.6	0.10
122	1100	300001	1000	F5 I	3.822	0.47	0.27	0.18	0.39	0.66	0.76	0.77	0	-6.6	0.07
123	1101	200001	0000	F8 I	3.785	1.00	0.60	0.28	0.50	0.86	1.14	1.20	0	-6.6	0.08
124	3001	110002	0010	G0 I	3.741	1.21	0.78	0.38	0.67	1.04	1.37	1.46	0	-6.6	0.00
125	3001	300012	1100	G2 I	3.724	1.51	0.90	0.42	0.75	1.16	1.48	1.49	0	-6.5	-0.02
126	3002	100001	0000	G5 I	3.703	1.86	1.07	0.47	0.83	1.32	1.71	1.80	0.1	-6.5	-0.09
127	1101	210000	1010	G8 I	3.662	2.35	1.21	0.59	1.01	1.48	1.77	1.81	0.0	-6.5	-0.18
128	3000	110001	1000	K2 I	3.629	3.10	1.50	0.70	1.26	1.85	2.18	2.27	-0.2	-6.6	-0.40
129	3001	110021	1000	K3 I	3.616	3.23	1.57	0.78	1.39	2.18	2.74	2.83	-0.1	-6.6	-0.63

TABLE 2—*Continued*

N	Components ^a			Type ^c	Log T _e	U ₃ -V	B ₃ -V	V-R _c	V-I _c	V-J	V-H	V-K	[Fe/H] ^d	M _{bol}	BC _V ^e
	^b sigk	jspnrd	ldkc												
130	3002	000021	1110	K4 I	3.601	3.34	1.66	0.84	1.63	2.74	3.45	3.65	-0.2	-6.7	-1.04
131	3001	310001	2210	M2 I	3.538	3.48	1.73	1.06	2.24	3.32	3.97	4.29	0	-8.3	-1.57

^aFor each library spectrum, the number of input spectra used from each of the first 14 Sources listed in table 1.

^bFor input spectra from Sviderskiene (1988) listed in the first column: 1) indicates a spectrum used to check the SED, but not included in the combination; 2) indicates the average of two spectra used similarly; 3) indicates a spectrum that was actually used in the combination, generally in the uv, and 4) indicates the average of two spectra used similarly.

^cA prefix “w” indicates metal-weak abundance; prefix “r” indicates metal-rich abundance.

^dAbundance estimated from the Mgb/MgH and Fe blend features.

^e $M_V = M_{bol} - BC_V$

^fThe Fluks et al. (1994) spectra are included in the M-giant library spectra only.

Fig. 1.— An example of the spectral combination process for the G2 V UVILIB component. As listed for component number 26 in table 2, this includes one reference SED spectrum from Sviderskiene (1988, the dotted line shown offset by 0.3 here, but not included in the combination), one IUE spectrum from Heck et al. (1984), one from Gunn and Stryker (1983) which is used in the blue and red, two from Kiehling (1987, with a formal RMS error on their individual average of 1.1%), two from Jacoby, Hunter and Christian (1984, RMS: 1.4%), one from Silva and Cornell (1992), one from Serote Roos, Boisson and Joly (1996) and one from Danks and Dennefeld (1994). Vertical lines indicate the start and end wavelength regions of the various components, together with atmospheric regions explicitly set zero. The final combination spectrum, which is the average of all non-zero contributions, is shown offset (by 0.8) above, and the standard deviation curve from the combination shown at bottom, with a formal RMS error of 0.9% over the full wavelength range.

Fig. 2.— Example UVILIB spectra showing the metallicity range for the G0 V components. The metal-weak library spectra represent stars about one-half solar metallicity, and the metal-rich spectra represent stars about twice solar metallicity. The strengths of the Balmer lines ($H\delta$ 4101, $H\gamma$ 4340 and $H\beta$ 4861) decrease while the strengths of the MgH/Mgb feature at 5175 Å and Fe I blends ($\lambda\lambda$ 4385, 5270, 5330 Å) increase going from metal-weak to metal-rich.

Fig. 3.— An example of the infrared spectral combination process for the K5 III UVKLIB component. This includes the pre-formed UVILIB K5 III spectrum, three spectra from Lancon and Rocca-Volmerange (1992, with a formal RMS error on their individual average of 1.9%), three from Dallier, Boisson and Joly (1996, RMS: 1.6%) one from Kleinmann and Hall (1986) and one from Cohen et al. (1996a) which is used here between 1.22–1.45 μm and at 2.5 μm . The crosses show the infrared flux points through which a smooth curve is fitted. This curve is included in the combination between 1.03–1.25 μm . The curve at the bottom shows the standard deviation of the individual average from 1.43–2.02 μm , and of the combination of averages to longer wavelengths.

Fig. 4.— Examples of the UVKLIB library. The K giant spectra include a smooth fit between 10500–

14300 Å, whereas the M giant spectrum includes data from Fluks et al. (1994) over this region.

Fig. 5.— Evolutionary points (EPs: small filled squares) for a solar-age, solar-metallicity isochrone from Bertelli et al. (1994), plotted as bolometric magnitude vs. $\text{Log } T_e$, with the library flux points overplotted and distinguished by metallicity and luminosity class. Not all the White Dwarf EPs are shown.

Fig. 6.— Three solar-age (5-Gyr) isochrones (lines) from Bertelli et al. (1994), of metal and helium abundance ($Z=0.008$, $Y=0.25$), ($Z=0.02$, $Y=0.28$) and ($Z=0.05$, $Y=0.352$) are plotted as absolute magnitude vs. $V-I_c$ color. The three isochrones illustrate the range of metallicity expected in composite populations. The G–K dwarf, subgiant and giant library points of metal-weak, solar and metal-rich abundance are overplotted, with the same symbol definition as in figure 5.

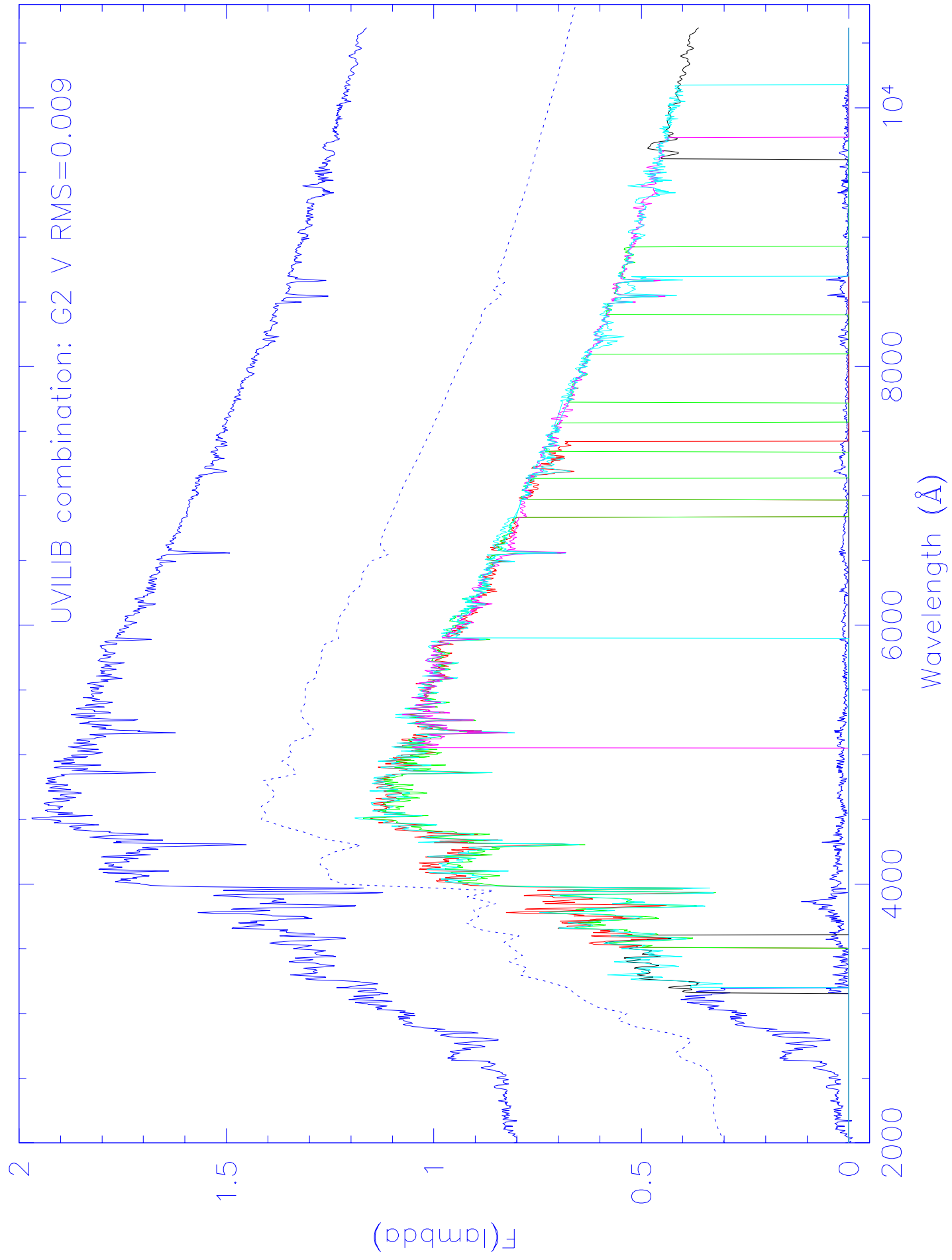
Fig. 7.— The isochrone EPs (crosses) extended to lower mass on the main sequence, with the library flux component points (same symbols as figure 5) overplotted and sized according to (a) the V-light fractions, and (b) the K-light fractions emitted by each component. Symbols at some important evolutionary phase changes represent fractional spectra interpolated between appropriate library components to accurately match the inflection in temperature (and luminosity).

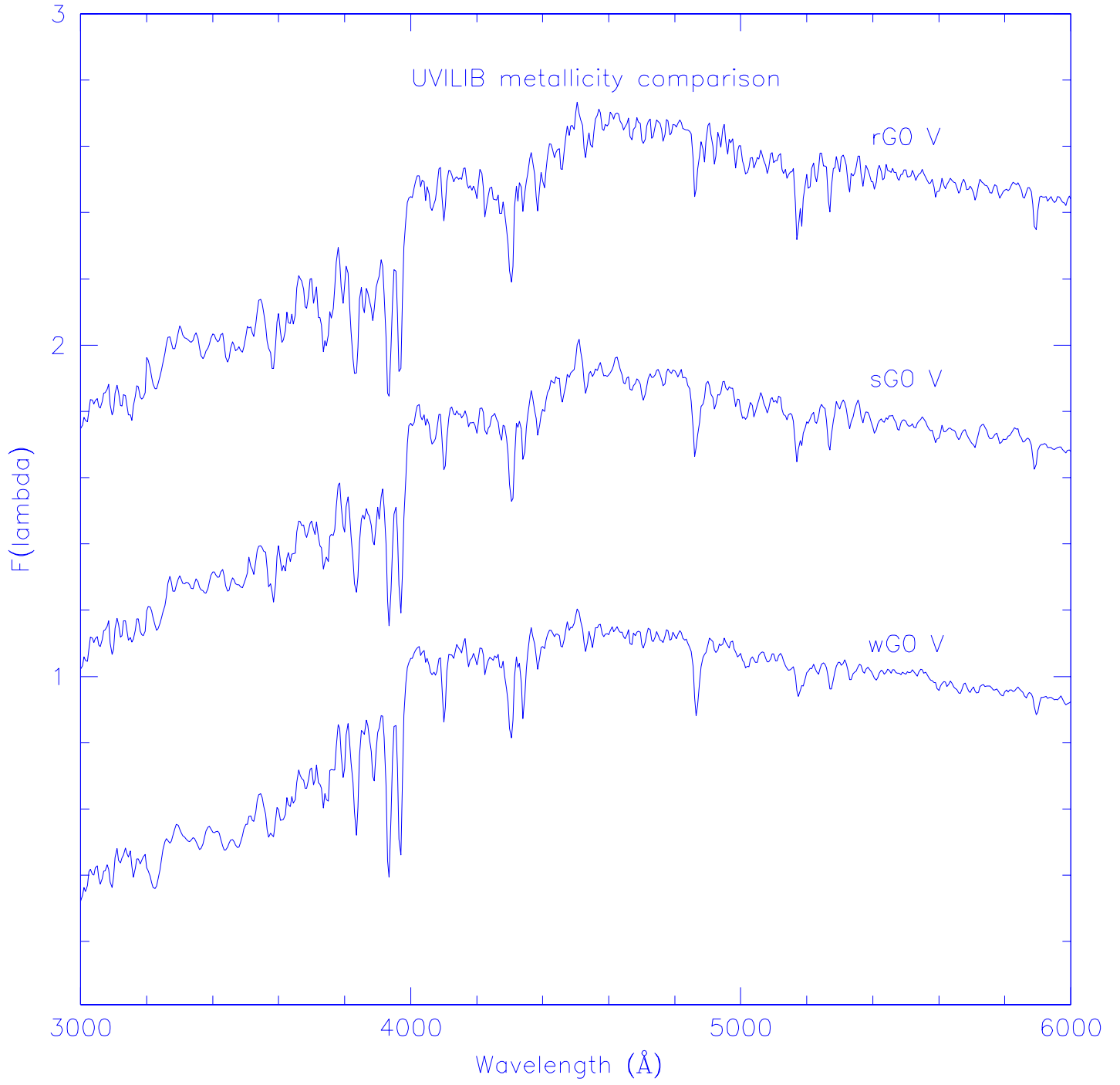
Fig. 8.— The library spectra co-added in the ratios determined from the previous figure. Spectra are grouped into lower main sequence (LMS – KM dwarfs), upper main sequence (UMS – FG dwarfs), subgiant (IV), first giant branch (GB – K-M7 giants), second and third giant branches (AGB – K-M9 III) and post asymptotic giant branch (PAGB), which is primarily contributed by an EP at $\text{Log } T_e=4.29$ and represented here by a combination of black body spectra. The top trace is the sum of the six components, and represents the emergent spectrum of a single-burst stellar population of solar-age and solar-metallicity.

REFERENCES

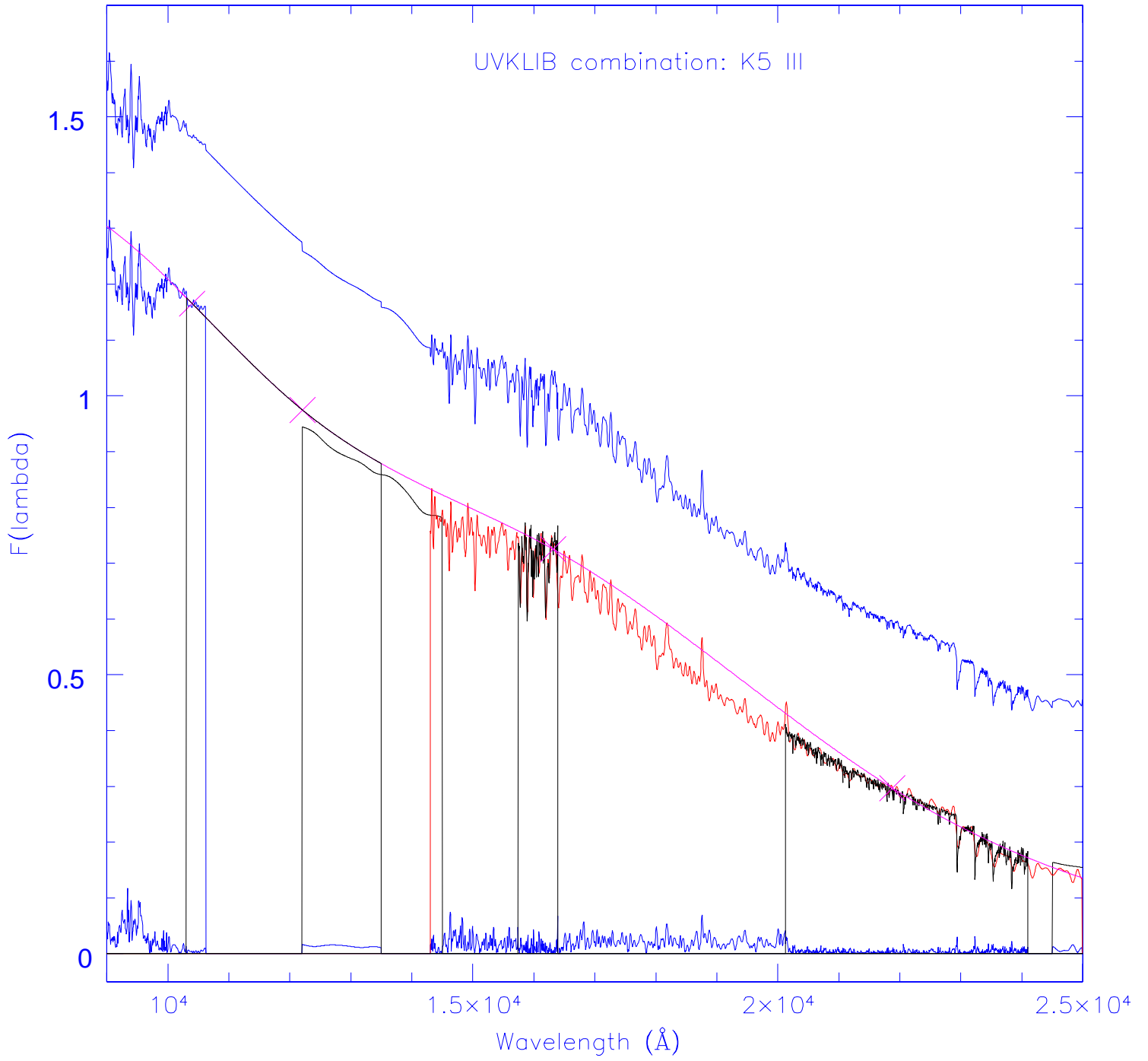
- Ažusienis, A., and Straizys, V. 1969, *Soviet Ast.*, 13, 316
- Bertelli, G., Bressan, A., Chiosi, C., Fagotto, F., and Nasi, E. 1994, *A&AS*, 106, 275
- Bessell M. S. 1979, *PASP*, 91, 589
- Bessell, M. S., and Brett, J. M. *PASP*, 100, 1134
- Bessell, M. S., and Wood, P. R. *PASP*, 96, 247
- Buser, R. 1978, *A&A*, 62, 411
- Charlot, S., Worthey, G., and Bressan, A. 1996, *ApJ*, 457, 625
- Cohen, M., Witteborn, F. C., Walker, R. G., Bregman, J. D., and Wooden, D. H. 1995, *AJ*, 110, 275
- Cohen, M., Witteborn, F. C., Bregman, J. D., Wooden, D. H., Salama, A., and Metcalfe, L. 1996, *AJ*, 112, 241
- Cohen, M., Witteborn, F. C., Carbon, D. F., Davies, J. K., Wooden, D. H., and Bregman, J. D. 1996, *AJ*, 112, 2274
- Cousins, A. W. J. 1981 SAAO circular no. 6, p4
- Dallier, R., Boisson, C., and Joly, M. 1996, *A&A*, 116, 239
- Danks, A. C., and Dennefeld, M. 1994, *PASP*, 106, 382
- Faber, S. M, Friel, E. D., Burstein, D., and Gaskell, C. M. 1985, *ApJS*, 57, 711
- Fluks, M. A., Plez, B., Thé, P. S., de Winter, D., Westerlund, B. E., and Steenman, H. C. 1994, *A&AS*, 105, 311
- Fluks, M. A., Plez, B., Thé, P. S., de Winter, D., Westerlund, B. E. and Steenman, H. C. 1997, (in preparation)
- Gunn, J. E., and Stryker, L. L. 1983, *ApJS*, 52, 121
- Hayes, D. S., and Latham, D. W. 1975, *ApJ*, 197, 593
- Heck, A., Egret, D., Jaschek, M., and Jaschek, C. 1984, *ESA SP-1052*
- Jacoby, G. H., Hunter, D. A., and Christian, C. A. 1984, *ApJS*, 56, 257
- Jones, L. A., and Worthey, G. 1995, *ApJ*, 446, L31
- Kiehling, R. 1987, *A&A*, 69, 465
- Kleinmann, S. G., and Hall, D. N. B. 1986, *ApJS*, 62, 501
- Koornneef, J. 1983, *A&A*, 128, 84
- Lancon, A., and Rocca-Volmerange, B. 1992, *A&A*, 96, 593
- Lang, K. R., *Astrophysical Data*, 1992, Springer-Verlag, New York.
- Leitherer, C. et. al. 1996, *PASP*, 108, 996
- Lupton, R. H., and Monger, P. 1997, *The SM Reference Manual*, <http://www.astro.princeton.edu/~rhl/sm/sm.html>
- Miller, G., and Scalo, J. 1979, *ApJS*, 41, 513
- Pickles, A. J. 1985, *ApJS*, 59, 33
- Pickles, A. J., and van der Kruit, P. C. 1990, *A&A*, 84, 421
- Rose, J. A. 1994, *AJ*, 107, 206
- Salpeter, E. E. 1955, *ApJ*, 121, 161
- Serote Roos, M., Boisson, C., and Joly, M. 1996, *A&A*, 117, 93
- Silva, D. R., and Cornell, M. E. 1992, *ApJS*, 81, 865
- Straizys, V., and Sviderskiene, S. 1972, *Bull. Vilna. Astron. Obs.*, 35, 23
- Sviderskiene, Z. 1988, *Bull. Vilna. Astron. Obs.*, 80, 1
- Tokunaga, A. T. 1997, *Astrophysical Quantities*, Revised, 4th Edition, ed. A. Cox, in press.
- Torres-Dodgen, A. V., and Weaver, W. B. 1993, *PASP*, 105, 693
- Whitford, A. E., and Rich, R. M. 1983, *ApJ*, 274, 723

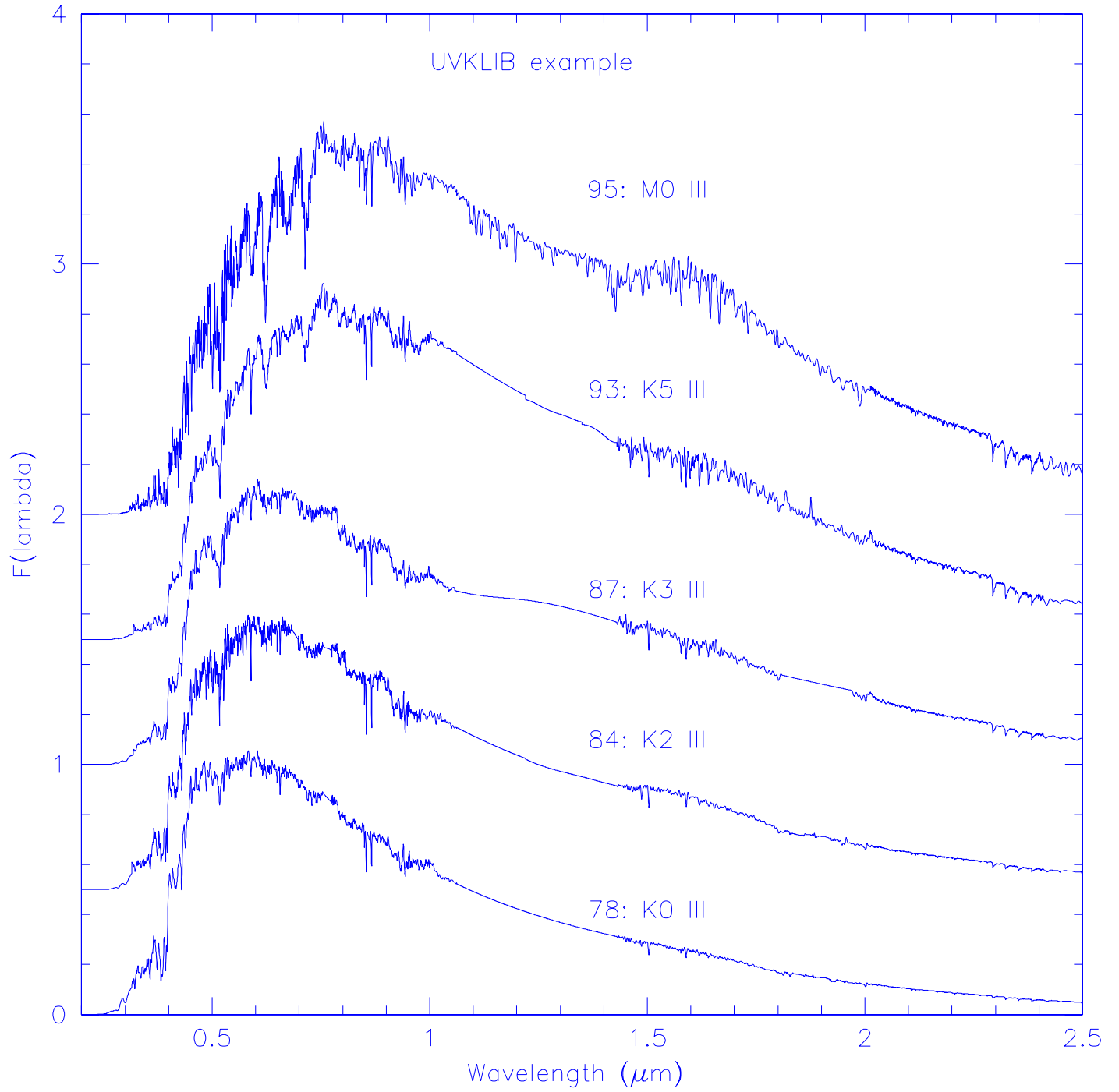
This 2-column preprint was prepared with the AAS L^AT_EX macros v4.0.

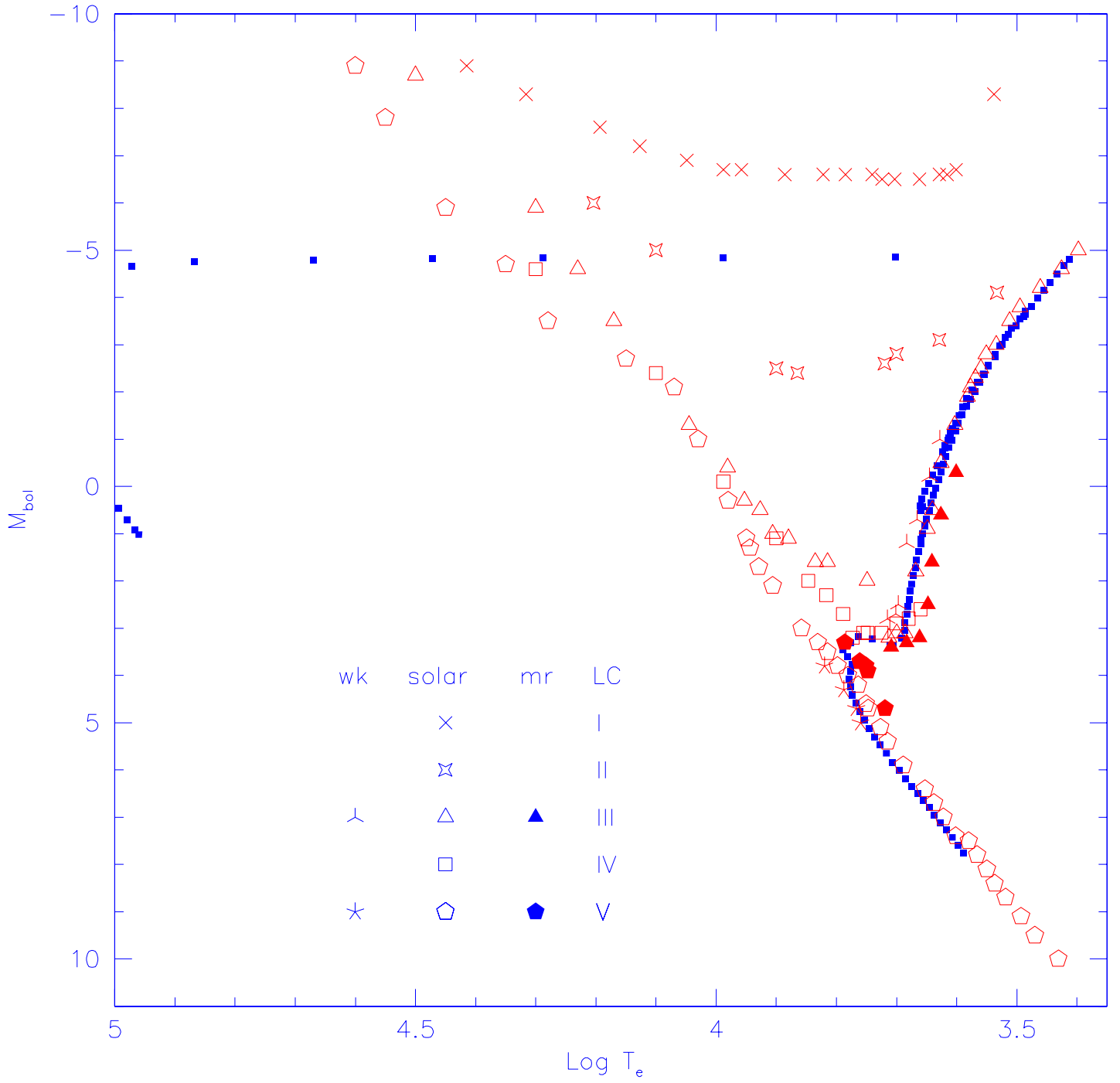




UVKLIB combination: K5 III







Solar 5Gyr Single Burst

